Received: 28 August 2023 | Revised: 25 October 2023 | Accepted: 12 November 2023

DOI: 10.1002/pro.4838

RESEARCH ARTICLE

THE PROTEIN SOCIETY WILEY

Nanoscale structural characterization of transthyretin aggregates formed at different time points of protein aggregation using atomic force microscopy-infrared spectroscopy

Axell Rodriguez[1] | **Abid Ali**[1] | **Aidan P. Holman**[2] | **Tianyi Dou**[1] | **Kiryl Zhaliazka**[1] | **Dmitry Kurouski**[1,3]

[1]Department of Biochemistry and Biophysics, Texas A&M University, College Station, Texas, USA

[2]Department of Entomology, Texas A&M University, College Station, Texas, USA

[3]Department of Biomedical Engineering, Texas A&M University, College Station, Texas, USA

Correspondence
Dmitry Kurouski, Department of Biomedical Engineering, Texas A&M University, College Station, TX 77843, USA.
Email: dkurouski@tamu.edu

Funding information
NIGMS, Grant/Award Number: R35GM142869

Review Editor: Jean Baum

Abstract

Transthyretin (TTR) amyloidosis is a progressive disease characterized by an abrupt aggregation of misfolded protein in multiple organs and tissues TTR is a tetrameric protein expressed in the liver and choroid plexus. Protein misfolding triggers monomerization of TTR tetramers. Next, monomers assemble forming oligomers and fibrils. Although the secondary structure of TTR fibrils is well understood, there is very little if anything is known about the structural organization of TTR oligomers. To end this, we used nano-infrared spectroscopy, also known as atomic force microscopy infrared (AFM-IR) spectroscopy. This emerging technique can be used to determine the secondary structure of individual amyloid oligomers and fibrils. Using AFM-IR, we examined the secondary structure of TTR oligomers formed at the early (3–6 h), middle (9–12 h), and late (28 h) of protein aggregation. We found that aggregating, TTR formed oligomers (Type 1) that were dominated by α-helix (40%) and β-sheet (∼30%) together with unordered protein (30%). Our results showed that fibril formation was triggered by another type of TTR oligomers (Type 2) that appeared at 9 h. These new oligomers were primarily composed of parallel β-sheet (55%), with a small amount of antiparallel β-sheet, α-helix, and unordered protein. We also found that Type 1 oligomers were not toxic to cells, whereas TTR fibrils formed at the late stages of protein aggregation were highly cytotoxic. These results show the complexity of protein aggregation and highlight the drastic difference in the protein oligomers that can be formed during such processes.

KEYWORDS

AFM-IR, fibrils, LDH, oligomers, transtherytin

1 | INTRODUCTION

Transthyretin (TTR) is a small tetrameric protein that transports thyroxine (T4), a thyroid hormone linked to metabolism, muscle and heart function, and brain development (Blake et al., 1978; Kanda et al., 1974; Saraiva et al., 2012; Yee et al., 2019). Under pathological conditions that are known as TTR amyloidosis, TTR deposits are found in various organs and tissues (Ando et al., 2005; Pires et al., 2012; Robinson & Reixach, 2014; Sanguinetti et al., 2022; Sebastiao et al., 2001). Although the exact cause of TTR amyloidosis is unclear, in vitro studies demonstrated that TTR aggregation is triggered by irreversible dissociation of the tetramer into monomers. Next, unfolded TTR monomers assembly into protein oligomers that later propagate into amyloid fibrils (Matsuzaki et al., 2017; Reixach et al., 2004).

Steinebrei et al. (2022) utilized cryo-electron microscopy (cryo-EM) to resolve the secondary structure of ex vivo extracted TTR fibrils. It was found that TTR fibrils were composed of several monomers that adopted β-sheet secondary structure that propagated in the direction perpendicular to β-strands. Similar experimental results were reported by Schmidt et al. (2019) for Val30Met mutant of TTR. These results are consistent with the secondary structure of amyloid fibrils adopted by other amyloidogenic proteins, including amyloid β (Aβ) and α-synuclein (α-syn) (Gremer et al., 2017; Guerrero-Ferreira et al., 2018; Heberle et al., 2020; Kollmer et al., 2019; Li et al., 2018). At the same time, there is very little if anything is known about the oligomers of such proteins (Chen et al., 2015; Knowles et al., 2014). Morphological heterogeneity and transient nature of such oligomers limit the use of cryo-EM and solid-state nuclear magnetic resonance for their structural characterization. Recently reported results by our and other research groups demonstrated that this problem can be overcome by atomic force microscopy-infrared (AFM-IR) spectroscopy (Dazzi, 2009; Dou et al., 2021; Ramer et al., 2018; Ruggeri et al., 2015; Ruggeri, Mannini, et al., 2020).

This innovative spectroscopic approach is based on the pulsed tunable IR light that is directed into the sample of interest (Centrone, 2015; Dazzi et al., 2010; Dazzi & Prater, 2017; Dou et al., 2020; Mayet et al., 2013; Ramer et al., 2017; Wieland et al., 2019). This causes thermal expansions in the illuminated specimens that are passed to the metalized scanning probe which can be positioned directly at the object of interest (Chae et al., 2017; Schwartz et al., 2022). Next, the thermal expansions are converted into IR spectra that can be used to interpret the secondary structure of individual oligomers or fibrils (Matveyenka et al., 2022b, 2022c; Rizevsky, Zhaliazka, et al., 2022; Ruggeri et al., 2015, 2016; Ruggeri, Benedetti, et al., 2018; Ruggeri, Charmet, et al., 2018; Ruggeri, Flagmeier, et al., 2020; Ruggeri, Mannini, et al., 2020) Using AFM-IR, Zhou and Kurouski (2020) found that α-syn oligomers found at the early time points of protein aggregation had a mixture of parallel and antiparallel β-sheet. However, α-syn oligomers found at the late stage of protein aggregation, as well as α-syn fibrils, were dominated by parallel β-sheet secondary structure. These results indicated that a conversion of antiparallel into parallel β-sheet was taken place upon oligomer growth and propagation into amyloid fibrils (Zhou & Kurouski, 2020). Zhaliazka and Kurouski (2022) found that $A\beta_{1-42}$ oligomers with parallel and antiparallel β-sheet had unequal rates of formation. Specifically, $A\beta_{1-42}$ had a much faster assembly rate forming parallel β-sheet oligomers compared to the oligomers with antiparallel β-sheet.

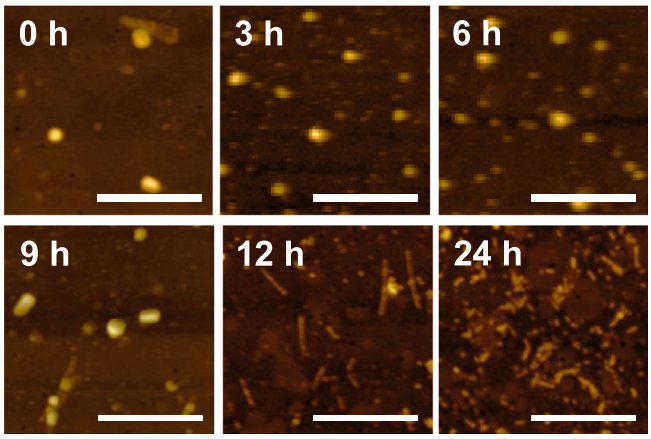

FIGURE 1 AFM images of TTR tetramers (0 h), oligomers (3–9 h), as well as oligomers and fibrils found at 12 and 24 h of protein aggregation at pH 3. Scale bars are 500 nm. AFM, atomic force microscopy; TTR, transthyretin.

In this study, we used AFM-IR to investigate the secondary structure of individual TTR oligomers formed at 3, 6, 9, 12, and 24 h of protein aggregation at pH 3. We also investigated the secondary structure of TTR fibrils formed at 9, 12, and 24 h. Finally, we used cell assays to determine the extent to which these protein aggregates exert cell toxicity to N27 rat dopaminergic cells.

2 | RESULTS

2.1 | Morphological transformations that are taking place upon TTR aggregation

AFM is a robust and reliable technique that is commonly used to monitor changes in the morphology of protein

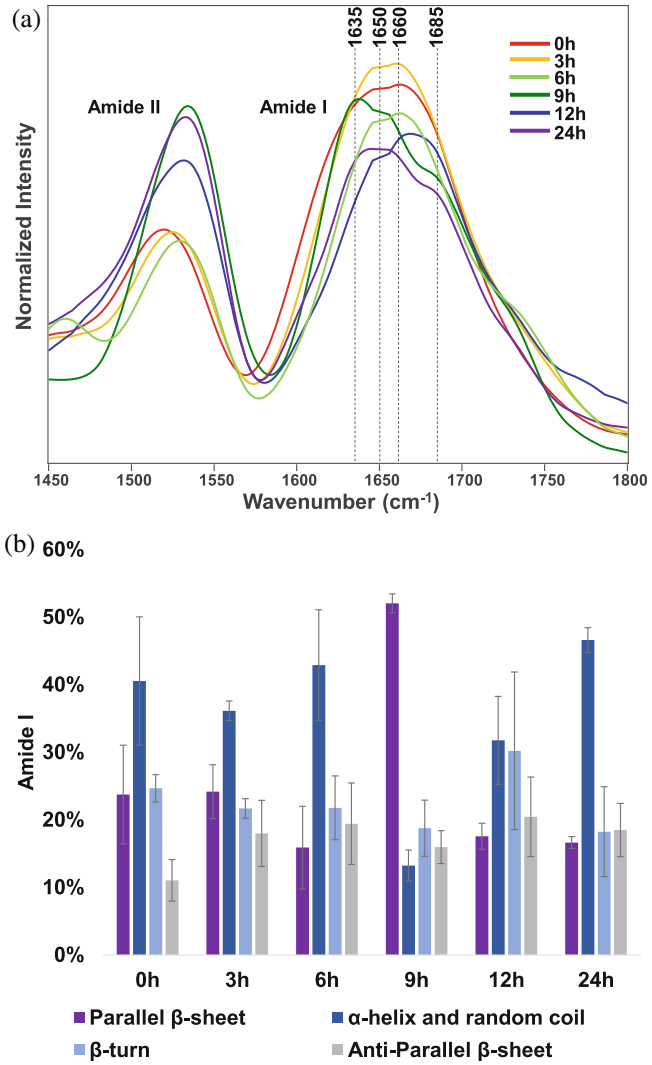

FIGURE 2 Averaged AFM-IR spectra acquired from TTR tetramers (0 h, red) and oligomers (a) formed at 3 h (orange), 6 h (light green), 9 h (green), 12 h (blue), and 24 h (purple). Histogram (b) of distribution of parallel and antiparallel β-sheet, α-helix, and unordered protein in TTR tetramers (0 h) and oligomers formed at the different time points of protein aggregation. AFM-IR, atomic force microscopy infrared; TTR, transthyretin.

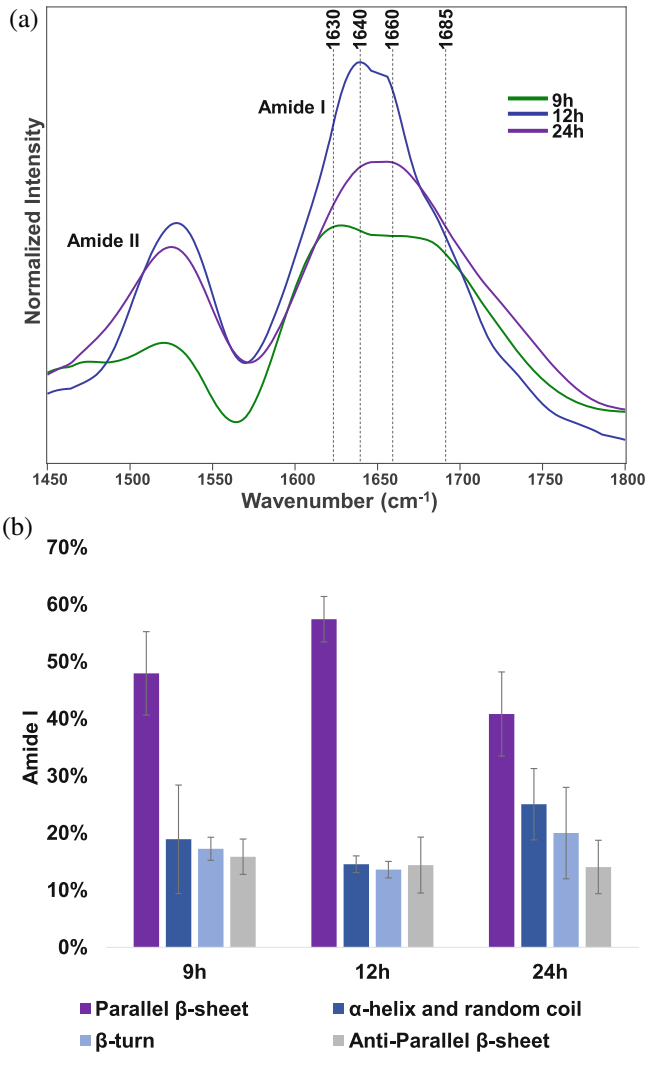

FIGURE 3 Averaged AFM-IR spectra acquired from TTR fibrils observed at 9 h (green), 12 h (blue), and 24 h (purple). Histogram (b) of distribution of parallel and antiparallel β-sheet, α-helix, and unordered protein in TTR fibrils formed at the different time points of protein aggregation. AFM-IR, atomic force microscopy infrared; TTR, transthyretin.

species that take place during their self-assembly into oligomers and fibrils (Ruggeri et al., 2019; Zhaliazka et al., 2023). Prior to the aggregation (0 h), TTR tetramers with heights of 8–12 nm were primarily observed (Figures 1 and S1). Only a very small number of higher-order aggregates (16–28 nm) were found in the 0 h sample.

At the early stage of protein aggregation (3–9 h), we primarily observed TTR oligomers with no fibrillar species detected. The heights of these oligomers ranged from 4 to 38 nm (3–9 h) (Figures 1 and S1). At the middle stage (12 h), we observed small fibrillar species together with the oligomers. The height of the fibrillar species ranged from 2.5 to 4.5 nm, whereas slightly thicker fibrils (5.5–9.5 nm) were observed (Figures 1 and S1). AFM imaging revealed a substantial increase in the abundance of fibrillar species at the late stage of TTR aggregation (24 h). It should be noted that the heights of fibrils observed at 24 h were larger (11–19 h) compared to the fibrils observed at 12 h of protein aggregation (5.5–9.5 nm) (Figures 1 and S1).

These findings suggested that tetramer dissociation and the assembly of TTR monomers into oligomers occurred within the first 6 h of protein aggregation. At the later time points (12 h), TTR oligomers propagated into fibrils. These findings are in good agreement with the kinetics of TTR aggregation recorded using thioflavin

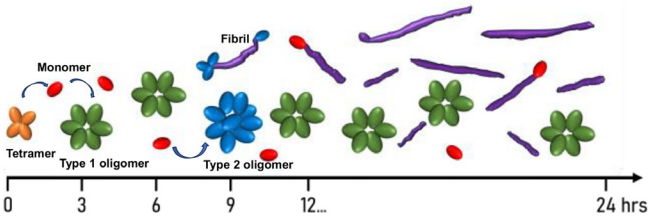

SCHEME 1 At pH 3, TTR tetramers dissociate into monomers that form Type 1 oligomers. These stable oligomers persist at later time points of TTR aggregation. At 9 h, Type 2 oligomers are formed that instantaneously propagate into fibrils. TTR, transthyretin.

T (ThT) assay (Figure S2). Thus, our results also revealed dynamic changes in the size of oligomers observed during the entire course of protein aggregation. However, AFM was not capable of probing changes in the secondary structure of TTR oligomers associated with the discussed above morphological transformations. To overcome this limitation, we used AFM-IR.

2.2 | Changes in the secondary structure of TTR oligomers and fibrils that take place during TTR aggregation

We acquired AFM-IR spectra from TTR tetramers at 0 h, as well as protein oligomers formed at 3, 6, 9, 12, and 24 h (Figures 3a,b and S3–S8). AFM-IR spectra exhibited amide I and II bands centered around 1525 and 1640 cm^{-1}, respectively (Figure 2). The position of the amide I band can be used to determine the secondary structure of analyzed specimens (Rizevsky, Matveyenka, & Kurouski, 2022). Specifically, the amide I band centered ~1635 cm^{-1} indicates the predominance of parallel β-sheet, whereas the amide I band around 1690 cm^{-1} indicates the antiparallel β-sheet in analyzed protein samples. Unfolded proteins exhibit amide I around 1660 cm^{-1}, whereas α-helical proteins had amide I ~1650 cm^{-1} (Matveyenka et al., 2022a, 2023). Expanding upon this, we fitted the acquired spectra to quantify the amounts of parallel and antiparallel β-sheet, α-helix, and unordered protein in the analyzed TTR oligomers.

We found very little if any changes in the secondary structure of TTR oligomers observed at 3 h compared to TTR tetramers that were present at 0 h of protein aggregation. Both types of protein specimens were dominated by α-helix (40%) and β-sheet (~30%) together with unordered protein (30%). Structurally similar oligomers were observed at 6 h. However, we found that oligomers formed at 9 h were drastically different from the oligomeric species observed at the early time points of protein

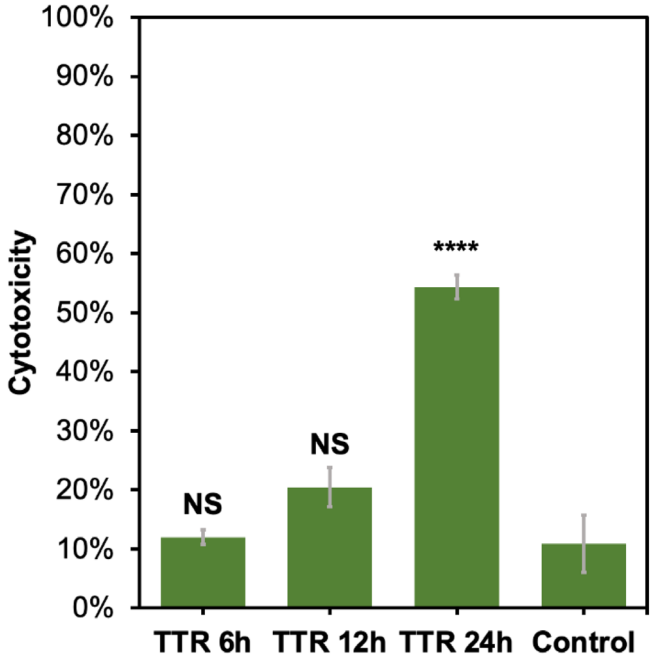

FIGURE 4 A histogram of LDH toxicity assay of TTR aggregates formed at 6, 12, and 24 h of protein aggregation. One-way ANOVA showed significant differences between samples ($p < 0.05$), and Tukey HSD post hoc test was used for further group comparison. ANOVA, analysis of variance; HSD, honest significant difference; LDH, lactate dehydrogenase; TTR, transthyretin.

aggregation. These new oligomers were primarily composed of parallel β-sheet (55%), with a small amount of antiparallel β-sheet, α-helix, and unordered protein. At this time point of protein aggregation, we also observed fibrillar species with the same secondary structure as the new oligomers (Figure 3a,b). Thus, one can expect that once formed, such β-sheet-rich oligomers rapidly propagated into fibrils. We also found that TTR oligomers observed at 12 and 24 h were structurally similar to the oligomers formed at 6 h of protein aggregation. These results indicate that TTR aggregation at the early time points (3–6 h) results in the formation of oligomers (Type 1) that are very similar to TTR tetramers from the perspective of their secondary structure (Scheme 1). Such oligomers persist unchanged at the later time points of protein aggregation (24 h). At the same time, later during the aggregation (9 h) a new class of oligomers is formed (Type 2). These oligomers are dominated by parallel β-sheet. Once formed, they instantaneously propagated into fibrils that were visible in the AFM images (9 h of TTR aggregation; Scheme 1). Such an abrupt propagation of these oligomers into fibrillar species was also confirmed by ThT kinetics (Figure S1).

It should be noted that we observed very little of any changes in the secondary structure of TTR fibrils formed at 12 and 24 h compared to the fibrils detected at 9 h

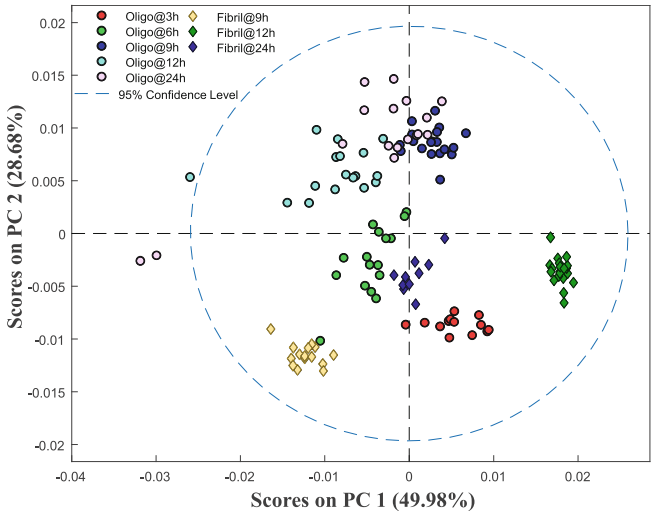

FIGURE 5 PCA plot of AFM-IR spectra acquired from oligomers and fibrils formed at different time points of protein aggregation. AFM-IR, atomic force microscopy infrared; PCA, principal component analysis.

(Figures 3 and S9–S11). All these protein aggregates were dominated by parallel β-sheet (42%–58%), with a small amount of antiparallel β-sheet, α-helix, and unordered protein (Figure 3).

2.3 | Toxicity of TTR aggregates formed at different time points of protein aggregation

We used N27 rat dopaminergic cells to investigate the relationship between protein aggregates observed at different time points of TTR aggregation and their toxicity. The cells were exposed to Type 1 oligomers formed at 6 h, as well as TTR aggregates formed at 12 and 24 h of protein aggregation (Figure 4). Next, a lactate dehydrogenase (LDH) assay was used to determine cell viability. We found that Type 1 oligomers formed at 6 h were not toxic to the N27 cells. At the same time, TTR fibrils formed at 24 h exerted strong cytotoxicity.

2.4 | Nano-infrared analysis of structural heterogeneity of TTR oligomers and fibrils

We used principal component analysis (PCA) to investigate the degree of structural heterogeneity of both oligomers and fibrils formed at different time points of protein aggregation (Figure 5; Zhaliazka & Kurouski, 2022). PCA revealed substantial diversity in the secondary structure of individual oligomers present at 12 and 24 h. At the same time, we observed only a small degree of structural heterogeneity in the TTR oligomers present at 3 h. TTR oligomers observed at 6 and 9 h exhibited lower structural heterogeneity than the oligomers detected at 12 and 24 h, but greater variability in their secondary structure than 3 h oligomers. These findings demonstrated that although on average very little structural transformations in these oligomers formed at different time points were observed (Figure 2), AFM-IR revealed a progressive increase in the structural variability of TTR oligomers from an early (3 h) to the late (12 and 24 h) time points.

AFM-IR coupled to PCA revealed significantly lower diversity in the fibrillar species observed at 9, 12, and 24 h compared to oligomers formed at these time points. Specifically, all fibrils observed at the same time point were found to be highly uniform from the perspective of their secondary structure (Figure 5).

3 | DISCUSSION

Protein aggregation is a complex process that follows free energy minimization (18; 5; 6). The process starts with protein misfolding which can be triggered by a large number of factors including low pH and high temperatures (Chiti & Dobson, 2017; Kurouski et al., 2010, 2014; Lai et al., 1996; Xu, Shashilov, Ermolenkov, et al., 2007; Xu, Shashilov, & Lednev, 2007). Previously reported results by the Kelly group demonstrated that low pH triggered monomerization of tetrameric TTR (Colon & Kelly, 1992; Kelly et al., 1997). Next, TTR monomers misfold and self-assembly into amyloid oligomers that later propagate into fibrils. Our results demonstrated that at least two types of TTR oligomers are formed as a result of protein aggregation. The first type is oligomers (Type 1) dominated by α-helix (40%) and β-sheet (∼30%) together with unordered protein (30%). These oligomers ranged from 18 to 38 nm. Nano-IR analysis of these oligomeric species revealed that such α-helix-rich oligomers were present not only at the early stages (3–6 h), but also at the late stages (12–24 h) of protein aggregation. We also found that the structural heterogeneity of such oligomers progressively increases with the duration of protein aggregation at pH 3. We also found that these Type 1 oligomers exert no cell toxicity. Similar results were reported by Zhaliazka and Kurouski (2022) for $A\beta_{1-42}$ oligomers formed at the early time points of protein aggregation. Independently, Rizevsky, Matveyenka, and Kurouski (2022) found that insulin oligomers formed at the early stages were far less toxic than insulin fibrils that were formed at the later stages of protein aggregation. Our results are in good agreement with the previously reported results by Rizevsky, Matveyenka, and Kurouski (2022). Specifically, we found that TTR fibrils that were

formed at 12 and 24 h were substantially more toxic than Type 1 oligomers formed at the early stages of protein aggregation (3–6 h). AFM-IR revealed that these fibrils were formed from completely different oligomers (Type 2) that were first observed only at 9 h. These new oligomers were dominated by parallel β-sheet (55%), with a small amount of antiparallel β-sheet, α-helix, and unordered protein. We also found that unlike protein oligomers, TTR fibrils observed at 12 and 24 h exhibited high structural similarities and very little if any heterogeneity. It should be noted that this complexity of protein aggregation cannot be revealed using conventional IR spectroscopy that probes a large volume of solution and, therefore, provides information about all types of aggregates present in the sample (Figure S12).

AUTHOR CONTRIBUTIONS

Dmitry Kurouski: Conceptualization; funding acquisition; writing – original draft; writing – review and editing; project administration; resources; supervision. **Axell Rodriguez:** Investigation; writing – review and editing; visualization; validation; methodology; formal analysis; data curation. **Abid Ali:** Investigation; methodology; validation; visualization; writing – review and editing; formal analysis; data curation. **Aidan P. Holman:** Investigation; methodology; validation; visualization; writing – review and editing; formal analysis; data curation. **Tianyi Dou:** Methodology; visualization; writing – review and editing; data curation; formal analysis. **Kiryl Zhaliazka:** Investigation; methodology; validation; visualization; writing – review and editing; data curation; formal analysis.

ACKNOWLEDGMENT

We are grateful to the NIGMS for the financial support (R35GM142869).

CONFLICT OF INTEREST STATEMENT

The authors declare no conflicts of interest.

ORCID

Dmitry Kurouski https://orcid.org/0000-0002-6040-4213

REFERENCES

Ando Y, Nakamura M, Araki S. Transthyretin-related familial amyloidotic polyneuropathy. Arch Neurol. 2005;62:1057–62.

Blake CC, Geisow MJ, Oatley SJ, Rerat B, Rerat C. Structure of prealbumin: secondary, tertiary and quaternary interactions determined by Fourier refinement at 1.8 A. J Mol Biol. 1978;121:339–56.

Centrone A. Infrared imaging and spectroscopy beyond the diffraction limit. Annu Rev Anal Chem. 2015;8:101–26.

Chae J, An S, Ramer G, Stavila V, Holland G, Yoon Y, et al. Nanophotonic atomic force microscope transducers enable chemical composition and thermal conductivity measurements at the nanoscale. Nano Lett. 2017;17:5587–94.

Chen SW, Drakulic S, Deas E, Ouberai M, Aprile FA, Arranz R, et al. Structural characterization of toxic oligomers that are kinetically trapped during alpha-synuclein fibril formation. Proc Natl Acad Sci USA. 2015;112:E1994–2003.

Chiti F, Dobson CM. Protein misfolding, amyloid formation, and human disease: a summary of progress over the last decade. Annu Rev Biochem. 2017;86:27–68.

Colon W, Kelly JW. Partial denaturation of transthyretin is sufficient for amyloid fibril formation in vitro. Biochemistry. 1992;31:8654–60.

Dazzi A. Photothermal induced resonance: application to infrared spectromicroscopy. In: Volz S, editor. Thermal nanosystems and nanomaterials. Berlin: Springer; 2009. p. 469–503.

Dazzi A, Glotin F, Carminati R. Theory of infrared nanospectroscopy by photothermal induced resonance. J Appl Phys. 2010;107:124519.

Dazzi A, Prater CB. AFM-IR: technology and applications in nanoscale infrared spectroscopy and chemical imaging. Chem Rev. 2017;117:5146–73.

Dou T, Li Z, Zhang J, Evilevitch A, Kurouski D. Nanoscale structural characterization of individual viral particles using atomic force microscopy infrared spectroscopy (AFM-IR) and tip-enhanced Raman spectroscopy (TERS). Anal Chem. 2020;92:11297–304.

Dou T, Zhou L, Kurouski D. Unravelling the structural organization of individual alpha-synuclein oligomers grown in the presence of phospholipids. J Phys Chem Lett. 2021;12:4407–14.

Gremer L, Scholzel D, Schenk C, Reinartz E, Labahn J, Ravelli RBG, et al. Fibril structure of amyloid-beta(1-42) by cryo-electron microscopy. Science. 2017;358:116–9.

Guerrero-Ferreira R, Taylor NM, Mona D, Ringler P, Lauer ME, Riek R, et al. Cryo-EM structure of alpha-synuclein fibrils. Elife. 2018;7:e36402.

Heberle FA, Doktorova M, Scott HL, Skinkle AD, Waxham MN, Levental I. Direct label-free imaging of nanodomains in biomimetic and biological membranes by cryogenic electron microscopy. Proc Natl Acad Sci USA. 2020;117:19943–52.

Kanda Y, Goodman DS, Canfield RE, Morgan FJ. The amino acid sequence of human plasma prealbumin. J Biol Chem. 1974;249:6796–805.

Kelly JW, Colon W, Lai Z, Lashuel HA, McCulloch J, McCutchen SL, et al. Transthyretin quaternary and tertiary structural changes facilitate misassembly into amyloid. Adv Protein Chem. 1997;50:161–81.

Knowles TP, Vendruscolo M, Dobson CM. The amyloid state and its association with protein misfolding diseases. Nat Rev. 2014;15:384–96.

Kollmer M, Close W, Funk L, Rasmussen J, Bsoul A, Schierhorn A, et al. Cryo-EM structure and polymorphism of Abeta amyloid fibrils purified from Alzheimer's brain tissue. Nat Commun. 2019;10:4760.

Kurouski D, Deckert-Gaudig T, Deckert V, Lednev IK. Surface characterization of insulin protofilaments and fibril polymorphs using tip-enhanced Raman spectroscopy (TERS). Biophys J. 2014;106:263–71.

Kurouski D, Lombardi RA, Dukor RK, Lednev IK, Nafie LA. Direct observation and pH control of reversed supramolecular chirality in insulin fibrils by vibrational circular dichroism. Chem Commun. 2010;46:7154–6.

Lai Z, Colon W, Kelly JW. The acid-mediated denaturation pathway of transthyretin yields a conformational intermediate that can self-assemble into amyloid. Biochemistry. 1996;35:6470–82.

Li B, Ge P, Murray KA, Sheth P, Zhang M, Nair G, et al. Cryo-EM of full-length alpha-synuclein reveals fibril polymorphs with a common structural kernel. Nat Commun. 2018;9:3609.

Matsuzaki T, Akasaki Y, Olmer M, Alvarez-Garcia O, Reixach N, Buxbaum JN, et al. Transthyretin deposition promotes progression of osteoarthritis. Aging Cell. 2017;16:1313–22.

Matveyenka M, Rizevsky S, Kurouski D. Amyloid aggregates exert cell toxicity causing irreversible damages in the endoplasmic reticulum. Biochim Biophys Acta Mol Basis Dis. 2022a;1868: 166485.

Matveyenka M, Rizevsky S, Kurouski D. Length and unsaturation of fatty acids of phosphatidic acid determines the aggregation rate of insulin and modifies the structure and toxicity of insulin aggregates. ACS Chem Nerosci. 2022b;13:2483–9.

Matveyenka M, Rizevsky S, Kurouski D. Unsaturation in the fatty acids of phospholipids drastically alters the structure and toxicity of insulin aggregates grown in their presence. J Phys Chem Lett. 2022c;13:4563–9.

Matveyenka M, Rizevsky S, Pellois JP, Kurouski D. Lipids uniquely alter rates of insulin aggregation and lower toxicity of amyloid aggregates. Biochim Biophys Acta Mol Cell Biol Lipids. 2023; 1868:159247.

Mayet C, Deniset-Besseau A, Prazeres R, Ortega JM, Dazzi A. Analysis of bacterial polyhydroxybutyrate production by multimodal nanoimaging. Biotechnol Adv. 2013;31:369–74.

Pires RH, Karsai A, Saraiva MJ, Damas AM, Kellermayer MS. Distinct annular oligomers captured along the assembly and disassembly pathways of transthyretin amyloid protofibrils. PLoS One. 2012;7:e44992.

Ramer G, Aksyuk VA, Centrone A. Quantitative chemical analysis at the nanoscale using the photothermal induced resonance technique. Anal Chem. 2017;89:13524–31.

Ramer G, Ruggeri FS, Levin A, Knowles TPJ, Centrone A. Determination of polypeptide conformation with nanoscale resolution in water. ACS Nano. 2018;12:6612–9.

Reixach N, Deechongkit S, Jiang X, Kelly JW, Buxbaum JN. Tissue damage in the amyloidoses: transthyretin monomers and nonnative oligomers are the major cytotoxic species in tissue culture. Proc Natl Acad Sci USA. 2004;101:2817–22.

Rizevsky S, Matveyenka M, Kurouski D. Nanoscale structural analysis of a lipid-driven aggregation of insulin. J Phys Chem Lett. 2022;13:2467–73.

Rizevsky S, Zhaliazka K, Dou T, Matveyenka M, Kurouski D. Characterization of substrates and surface-enhancement in atomic force microscopy infrared analysis of amyloid aggregates. J Phys Chem C Nanomater Interfaces. 2022;126:4157–62.

Robinson LZ, Reixach N. Quantification of quaternary structure stability in aggregation-prone proteins under physiological conditions: the transthyretin case. Biochemistry. 2014;53:6496–510.

Ruggeri FS, Benedetti F, Knowles TPJ, Lashuel HA, Sekatskii S, Dietler G. Identification and nanomechanical characterization of the fundamental single-strand protofilaments of amyloid alpha-synuclein fibrils. Proc Natl Acad Sci USA. 2018;115: 7230–5.

Ruggeri FS, Charmet J, Kartanas T, Peter Q, Chia S, Habchi J, et al. Microfluidic deposition for resolving single-molecule protein architecture and heterogeneity. Nat Commun. 2018;9:3890.

Ruggeri FS, Flagmeier P, Kumita JR, Meisl G, Chirgadze DY, Bongiovanni MN, et al. The influence of pathogenic mutations in alpha-synuclein on biophysical and structural characteristics of amyloid fibrils. ACS Nano. 2020;14:5213–22.

Ruggeri FS, Longo G, Faggiano S, Lipiec E, Pastore A, Dietler G. Infrared nanospectroscopy characterization of oligomeric and fibrillar aggregates during amyloid formation. Nat Commun. 2015;6:7831.

Ruggeri FS, Mannini B, Schmid R, Vendruscolo M, Knowles TPJ. Single molecule secondary structure determination of proteins through infrared absorption nanospectroscopy. Nat Commun. 2020;11:2945.

Ruggeri FS, Sneideris T, Vendruscolo M, Knowles TPJ. Atomic force microscopy for single molecule characterisation of protein aggregation. Arch Biochem Biophys. 2019;664:134–48.

Ruggeri FS, Vieweg S, Cendrowska U, Longo G, Chiki A, Lashuel HA, et al. Nanoscale studies link amyloid maturity with polyglutamine diseases onset. Sci Rep. 2016;6:31155.

Sanguinetti C, Minniti M, Susini V, Caponi L, Panichella G, Castiglione V, et al. The journey of human transthyretin: synthesis, structure stability, and catabolism. Biomedicines. 2022; 10:1906.

Saraiva MJ, Magalhaes J, Ferreira N, Almeida MR. Transthyretin deposition in familial amyloidotic polyneuropathy. Curr Med Chem. 2012;19:2304–11.

Schmidt M, Wiese S, Adak V, Engler J, Agarwal S, Fritz G, et al. Cryo-EM structure of a transthyretin-derived amyloid fibril from a patient with hereditary ATTR amyloidosis. Nat Commun. 2019;10:5008.

Schwartz JJ, Jakob DS, Centrone A. A guide to nanoscale IR spectroscopy: resonance enhanced transduction in contact and tapping mode AFM-IR. Chem Soc Rev. 2022;51:5248–67.

Sebastiao MP, Lamzin V, Saraiva MJ, Damas AM. Transthyretin stability as a key factor in amyloidogenesis: X-ray analysis at atomic resolution. J Mol Biol. 2001;306:733–44.

Steinebrei M, Gottwald J, Baur J, Rocken C, Hegenbart U, Schonland S, et al. Cryo-EM structure of an ATTRwt amyloid fibril from systemic non-hereditary transthyretin amyloidosis. Nat Commun. 2022;13:6398.

Wieland K, Ramer G, Weiss VU, Allmaier G, Lendl B, Centrone A. Nanoscale chemical imaging of individual chemotherapeutic cytarabine-loaded liposomal nanocarriers. Nano Res. 2019;12: 197–203.

Xu M, Shashilov V, Lednev IK. Probing the cross-beta core structure of amyloid fibrils by hydrogen-deuterium exchange deep ultraviolet resonance Raman spectroscopy. J Am Chem Soc. 2007;129:11002–3.

Xu M, Shashilov VA, Ermolenkov VV, Fredriksen L, Zagorevski D, Lednev IK. The first step of hen egg white lysozyme fibrillation, irreversible partial unfolding, is a two-state transition. Protein Sci. 2007;16:815–32.

Yee AW, Aldeghi M, Blakeley MP, Ostermann A, Mas PJ, Moulin M, et al. A molecular mechanism for transthyretin amyloidogenesis. Nat Commun. 2019;10:925.

Zhaliazka K, Kurouski D. Nanoscale characterization of parallel and antiparallel beta-sheet amyloid beta 1-42 aggregates. ACS Chem Nerosci. 2022;13:2813–20.

Zhaliazka K, Matveyenka M, Kurouski D. Lipids uniquely alter the secondary structure and toxicity of amyloid beta 1–42 aggregates. FEBS J. 2023;290:3203–20.

Zhou L, Kurouski D. Structural characterization of individual alpha-synuclein oligomers formed at different stages of protein aggregation by atomic force microscopy-infrared spectroscopy. Anal Chem. 2020;92:6806–10.

SUPPORTING INFORMATION

Additional supporting information can be found online in the Supporting Information section at the end of this article.

How to cite this article: Rodriguez A, Ali A, Holman AP, Dou T, Zhaliazka K, Kurouski D. Nanoscale structural characterization of transthyretin aggregates formed at different time points of protein aggregation using atomic force microscopy-infrared spectroscopy. Protein Science. 2023;32(12):e4838. https://doi.org/10.1002/pro.4838